



## ORIGINAL ARTICLE

# Innovative high-performance cement treated crushed stones as rolled concrete

*Inovadora brita graduada tratada com cimento de alto desempenho como concreto compactado com rolo*

Andréia Posser Cargini<sup>a</sup>

José Tadeu Balbo<sup>a</sup>

Liédi Legi Barianni Bernucci<sup>a,b</sup>

<sup>a</sup>Universidade de São Paulo, Escola Politécnica, Departamento de Engenharia de Transportes, São Paulo, SP, Brasil

<sup>b</sup>Instituto de Pesquisas Tecnológicas do Estado de São Paulo, São Paulo, SP, Brasil

Received 07 June 2023

Revised 26 August 2023

Accepted 16 November 2023

Corrected 27 March 2024

**Abstract:** The main causes of poor performance of cement-treated crushed stones (CTCS) pavement layers are material-related heterogeneity, porosity, and brittle cementitious matrix, leading to fast fatigue degradation. Seeking to improve CTCS mechanical properties and structural response it was studied different grading curves such as DER-SP, EN 14227-1 CBGM 2 and RCC-ACI were studied. The aim of the laboratory study was to rank and select among the classical particle size distribution models like Talbot & Richart, and analytical models as compressible packing model – CPM, the best grading curve which was capable of producing mixtures with the best aggregate interlocking and improved mechanical resistances. The effect of cement content (4% and 5%) as well as the potential of using silica fume in suspension (percentages of 5, 7 and 10% of cement mass) to improve the interfacial transition zone were evaluated. It was found that CPM is a powerful tool for aggregates ranking aggregates and designing well-graded mixtures like CTCS; the CBGM 2 EN 14227-1 mean curve achieved the best packing density. The effect of increasing the cement content from 4 to 5% in terms of mechanical strength has the same result as the addition of 7% of silica fume in mixtures with 4% cement. Eventually, mixtures with 5% cement and 10% silica fume showed modulus of elasticity similar to traditional CTCS; nonetheless, the HP-CTCS (high performance CTCS) split tensile strength was significantly higher (about 28%), leading to a lower  $E_{t,sp}/f_{ct,sp}$  relationship, which is a highly positive outcome to improve mechanical durability of this innovative dry compacted concrete.

**Keywords:** high performance cement-treated crushed stone, mechanical strength, aggregate packing, supplementary cementitious material, silica fume in suspension.

**Resumo:** As principais causas do desempenho insatisfatório de bases de brita graduada tratada com cimento (BGTC) está relacionada à sua matriz cimentícia heterogênea, porosa e frágil que favorece o processo de degradação por fadiga. Assim, buscando melhorar as propriedades mecânicas e resposta estrutural da BGTC, o presente estudo avaliou diferentes faixas granulométricas (DER-SP, CBGM 2 EN 14227-1 e CCR-ACI) através de modelos clássicos de distribuição de partículas como Talbot & Richart e modelo analítico do empacotamento compressível (*compressible packing model* – CPM) para classificar e selecionar curvas granulométricas capazes de potencializar o empacotamento das partículas e melhorar a resistência mecânica da mistura. O efeito do teor de cimento (4 e 5%) foi avaliado, bem como o potencial de se utilizar sílica ativa em suspensão (em porcentagens de 5, 7 e 10% da massa de cimento) para modificar a zona de transição interfacial. Verificou-se que o CPM é uma poderosa ferramenta para a seleção e projeto de misturas bem graduadas; a curva média para a faixa CBGM 2 da norma Europeia EN 14227-1 apresentou a maior densidade de empacotamento. O efeito do aumento do teor de cimento de 4% para 5%, em termos de resistência mecânica, poderia ser compensado pela adição de 7% de sílica ativa à mistura com 4% de cimento. Por fim, misturas com 5% de cimento e 10% de sílica ativa apresentaram valores de módulo de elasticidade muito similares àqueles tradicionalmente obtidos para BGTC; contudo, a resistência à tração indireta da BGTCAD foi significativamente maior (em torno de 28%), levando à uma relação modular ( $E_{t,sp}/f_{ct,sp}$ ) menor, o que é promissor em termos durabilidade mecânica para esse tipo de concreto seco.

**Corresponding author:** Andréia Posser Cargini. E-mail: andrea.cargini@usp.br

**Financial support:** CAPES – Ministry of Education, Brazil.

**Conflict of interest:** Nothing to declare.

**Data Availability:** the data the support the findings of this study are available from the corresponding author, [APC], upon reasonable request.

This document has an erratum: <https://doi.org/10.1590/S1983-41952024000500011>



This is an Open Access article distributed under the terms of the Creative Commons Attribution License, which permits unrestricted use, distribution, and reproduction in any medium, provided the original work is properly cited.

**Palavras-chave:** brita graduada tratada com cimento de alto desempenho, resistência mecânica, empacotamento dos agregados, materiais cimentícios suplementares, sílica ativa em suspensão.

**How to cite:** A. P. Carginin, J. T. Balbo, and L. L. B. Bernucci, “Innovative high-performance cement treated crushed stones as rolled concrete.” *Rev. IBRACON Estrut. Mater.*, vol. 17, no. 5, e17510, 2024, <https://doi.org/10.1590/S1983-41952024000500010>

## 1 INTRODUCTION

Stabilization of soils and granular materials has long been used in the 20<sup>th</sup> century by road engineers to improve the stiffness of base materials considered unsuitable for paving. Stabilization can be achieved by mixing different materials to change the grain size distribution or even by adding chemicals to the original material, or by combining both processes, to obtain mechanical benefits. The first is achieved by means of improvements of mixture gradation seeking to increase the aggregates interlocking; the second one is associated with the addition of a stabilizing agent such as a hydraulic binder, lime, some types of pozzolans and blast furnace slag activated by lime or cement [1]–[5].

York [1]–[12] defines as cement-bound materials the “[...] *granular material or soil mixed with cement and compacted at or about optimum moisture content by external vibration*” and separates the whole family in five categories covering since cement-stabilized soil mixtures up to roller compacted concrete, as illustrated in the Table 1.

**Table 1.** Range of cement-bound materials (adapted from York [6])

Type of mixture	Main material	Cement content (by weight)	Strength (7 days)	Cement effect
Cement stabilized soil	Soil	Less than 5%	CBR 15-30%	Partial improvements of material features, such as plasticity, water susceptibility and swelling.
Soil cement	Soil	Over 5%	Compressive strength 1-5 MPa	The crystals generated from the cement hydration create a skeleton which involves the soil particles and fix them, increasing the compressive and tensile strength of the mixture and stiffness as well.
Cement-bound granular materials (CBMG)	Well graded crushed stone	From 3 to 5%	Compressive strength 4-10 MPa	Limited to form connection points between the aggregates since the mortar content is scarce to involve the grains completely.
Lean concrete	Well graded crushed stone	Over 5% and less than 10%	Compressive strength 7-20 MPa	The volume of paste is higher than CBGM materials, creating a material with higher strength and stiffness, but the grading envelope is narrower than CBGM.
Roller compacted concrete (RCC)	Well graded crushed stone	Range from 10 to 17%	Compressive strength > 20 MPa	Relative stiff mixture of aggregates (maximum size not larger than 19 mm). Mixtures should have enough paste volume to fill the internal voids in the aggregate mass. Mixture can be designed regarding two proportioning methods: soil compaction tests and concrete consistency tests (Vebe apparatus). No mandatory enveloped grain size distribution.

In Brazil, cement stabilized materials have been used since 1950s, initially through soil-cement mixtures (in state of Sao Paulo). From 1967, it started the application of cement-treated crushed stones (CTCS; BGTC is the abbreviation in Portuguese) as base for asphalt pavements under heavy traffic. These mixtures still are produced with cement contents of 3% or 4% (cement consumption from 75 to 90 kg/m<sup>3</sup>). However, many road projects employing CTCS (as pavement base underneath asphalt layers) presented poor performance including premature failures and intense fatigue cracking propagation to the asphalt surfaces after about two years of traffic exposure [7]. This kind of problem with CTCS remains currently with records of cement-treated base fatigue life consumption 21 months after construction as recently observed at the BR-101 highway [8], [9].

It should be noted that restrictive compaction procedures are hardly specified for the CTCS standards. The reasons why pavements constructed with CTCS as a base have presented poor performance (early cracks), among other causes, are explained by the material porosity, heterogeneity and brittle cementitious matrix, which favor quick fatigue damage [10]. Pour design

failures in terms of CTCS thickness in face of truck loads were also identified in most cases. It is worth to emphasize that CTCS strength is an outcome of the combined effect of granular skeleton and cementitious matrix; the first effect is responsible for the mechanical stability of the mixture through aggregate interlocking and the second is accountable for tensile strength and stiffness development through bonding bridges connecting aggregate particles, promoted by cement hydrated products.

It is well documented in the technical literature that the higher the cement consumption, the higher the mechanical strength, as the amount of hydrated products is equally greater [2], [11]–[14]. However, it should be noted that this strength gain by increasing cement contents has relevant economic impact as well as the addition of silica fume emulsified, not quantified herein, beyond increasing undesirable drying shrinkage, which has represented a concerning factor for the use of cement-bound materials like RCC and CTCS for road construction.

From this background, it was identified needs of improving the CTCS performance seeking to achieve a more homogeneous matrix, bringing it closer to an RCC without significantly increasing its cement content as well as not significantly modifying its stiffness, an important factor for design of cemented base layers. Then, the desired improvements can be reached through aggregate grading improvements, favoring the interlocking between particles and mineral additions capable of improving the microstructure of the cementitious matrix, especially the interfacial transition zone (ITZ) between the aggregates and the cement paste. This interfacial transition is considered the weakest link in the chain because the cement content is low, generating reduced mortar volume within the matrix.

Cargnin et al. [15] investigated several grading curves for cement-treated materials embracing Brazilian specifications for CTCS like the ABNT NBR 11803 [16], DER-SP [17] and DER-PR [18], as well as international specifications such as the European Standard EN 14227-1 [19], the American Portland Cement Association (PCA) [20] and American Concrete Institute (ACI) [21] grading curves for cement-treated materials and RCC, respectively. Initially, the authors analyzed the grading curves through the Talbot coefficient and picked up three of them (DER-SP specification for CTCS, the ACI grading curve for RCC, and the EN 14227-1 CBGM 2 envelope) which were reproduced in the laboratorial study. The authors confirmed (for a significance level of 95%) that the size distribution has a significant impact on compressive and indirect tensile strength; the compressive and the indirect tensile strength were 20% and 10%, respectively, higher for CBGM 2 (EN 14227-1) compared to mixtures produced according to DER-SP specification and RCC (ACI specification).

Regarding mineral additions, it is known that supplementary cementitious materials like silica fume and pozzolans have positive impacts on mechanical properties of concretes, reducing the extension of the ITZ, making it less porous and increasing, consequently, the strength and durability of the concrete [22]–[24]. Marchand et al. [25] addressed that the cement paste fractions of concretes produced with low cement content ( $\leq 300 \text{ kg/m}^3$ ) is significantly less homogeneous than conventional concretes. However, the addition of silica fume and fly ash enhanced the homogeneity of the RCC paste. Vahedifard et al. [26], studying low-cement content RCC with the addition of silica fume obtained significantly higher compressive strengths than the reference concrete; for RCC with 12% cement and 10% silica fume, the increase of strength was around 19%, whilst for mixtures with 15% cement content the strength was 22% higher than the reference. This is an outcome of the silica fume contributing to ITZ densification through the filler effect (particles of silica fume are lower than  $1 \mu\text{m}$  refining the porous structure) and the chemical effect resulting from pozzolanic reactions (formation of additional C-S-H due to the reaction of  $\text{SiO}_2$  with the calcium hydroxide –  $\text{Ca(OH)}_2$ .)

Therefore, the main objective of this study is to discuss the formulation of a CTCS mixture with high performance namely HP-CTCS (BGTCAD, in Portuguese), regarding the granulometric distribution; the grading curve of interest was selected based on the analysis following classical particle size distribution models and an analytical model (Compressible Packing Model – CPM [27]). The effects of cement content and the potential of adding silica fume emulsion as an agent capable of modifying the ITZ are highlighted through analyzing the parameters such as compressive and indirect tensile strength, and modulus of elasticity, beyond measuring the HP-CTCS Poisson's ratio.

## 1.1 Grading curves analysis

Combining grains through particle packing models and techniques seeking to minimize porosity in cementitious materials has been a prevailing activity reported by several authors, since it allows the use of significantly smaller amounts of cement to produce mixtures without jeopardizing their mechanical parameters [27]–[31].

Several studies have reported the production of concretes with significantly lower cement consumption than conventional concretes using particle packing models to optimize the concrete proportioning [29], [31]–[33]. Although most of such models have been developed for plastic, self-compacting and ultra-high strength concretes, their application for cement-stabilized materials like CTCS becomes reasonable, especially considering the low cement consumption and relevance of the granular skeleton to the mechanical strength of this material.

### 1.1.1 Particle packing models

The development of well-graded mixtures for pavements like crushed stones, Portland cement concretes, cement-treated aggregate materials, and conventional hot mix asphalt (HMA) are based on the Fuller and Thompson [34] studies as well as Talbot and Richart [35], which describe a curve given by an exponent relation between the particle size and the maximum aggregate size, according to Equation 1.

$$p = 100 \cdot \left(\frac{d}{D}\right)^n \quad (1)$$

where  $p$  is the percentage by mass of particles passing through a sieve with diameter  $d$ ;  $d$  is the diameter of the considered sieve;  $D$  is the maximum aggregate size;  $n$  is the variable exponent also known as modulus distribution (maximum density attained for  $n = 0.50$ ).

Apart from this classical model, other studies proposed some changes in this approach. Andreassen and Andersen [36] and Funk and Dinger, as addressed by Kumar and Santhanam [32], proposed some adjustments in the classical model; the first study used the same Equation 1 but proposed an exponent range between 0.21 and 0.37 determined experimentally for plastic concretes; Vanderlei [37] highlights that for flowable concretes,  $n$  values should be below 0.30; self-compacting concretes, on the other hand, should present  $n$  lower than 0.23, whereas mixtures with  $n$  around 0.32 require vibration to attain a good densification, like roller compacted concretes [32].

Funk and Dinger [38] addressed that the classical model has a limitation regarding the minimum particle size, as it does not assume a minimum particle diameter as proposed in the following model (Equation 2):

$$p = \frac{d^n - d_{min}^n}{D^n - d_{min}^n} \quad (2)$$

where  $p$  is the percentage of particles passing through a sieve with diameter  $d$ ;  $D$  is the maximum particle size;  $d_{min}$  is the minimum particle size.

Although these models were developed for plastic, self-compacting and ultra-high strength concretes, their application to cement-stabilized materials are reasonable, especially considering the low cement content in CTCS and the relevance of aggregate skeleton to the material mechanical characteristics. Several studies have reported the production of concretes with reduced cement content using particle packing models to optimize the aggregates consumption and the volume of paste [29], [31]–[33].

Nevertheless, researchers have emphasized that the main issue with these models is the fact that they do not consider the effect of particle shape, as well as the interaction between larger and smaller grains and compaction effects [28], [29], [31], aspects considered in the analytical models.

Particle packing analytical models describe through mathematical equations how aggregate grains with different sizes interact between each other also considering their geometry. Several authors emphasize the compressible packing model (CPM) developed by Larrard [27] as the most complete among analytical models for packing optimization since it covers the interaction between any fraction and size distribution including the effect of densification type [28]–[32]. This model is based on the virtual packing density and the compaction index, seeking to predict the real packing density of a polydisperse mixture regarding the following parameters: (i) the packing density of each mono-sized aggregate class, (ii) the mixture size distribution and, (iii) the compaction energy.

In a mixture composed of  $n$  classes of mono-size particles separated through sieving process, it is necessary to know the packing density ( $\beta_i$ ) of each class  $i$ , experimentally determined knowing the specific mass ( $\rho_d$ ) and the unit mass ( $\rho_u$ ) as described by Equation 3:

$$\beta_i = 1 - \frac{\rho_d - \rho_u}{\rho_d} \quad (3)$$

The virtual packing density is then determined by Equation 4 as follows, and is the lowest value obtained for each  $i$  class, considered as dominant:

$$\gamma_i = \frac{\beta_i}{1 - \sum_{j=1}^{i-1} \left[ 1 - \beta_i + b_{ij} \times \beta_i \left( 1 - \frac{1}{\beta_j} \right) \right] \times y_j - \sum_{j=i+1}^n \left[ 1 - a_{ij} \times \frac{\beta_j}{\beta_i} \right] \times y_j} \tag{4}$$

where  $\gamma_i$  is the virtual packing density;  $\beta_i$  and  $\beta_j$  is the packing density for each particle class, being  $i$  the dominant class and  $j$  the other classes for each combination of particle sizes;  $y_j$  = volume of material normalized by the total sum of percentages passing from grading curve;  $a_{ij}$  and  $b_{ij}$  are the interaction effects between particles defined, respectively, as the loosening and wall effect.

The wall effect describes the action held by the coarse particles on the small grains, which causes a decrease in the packing density by increasing the porosity surrounding the large particles. The loosening effect, on the other hand, is the distance between particles caused by the small ones when they are too large to be positioned in the voids existing between coarser particles. These effects can be calculated by Equations 5 and 6 and are illustrated by Figure 1.

$$a_{ij} = \sqrt{1 - \left( 1 - \frac{d_j}{d_i} \right)^{1.02}} \tag{5}$$

$$b_{ij} = 1 - \left( 1 - \frac{d_i}{d_j} \right)^{1.5} \tag{6}$$

where  $a_{ij}$  is loosening effect;  $b_{ij}$  is the wall effect;  $d_i$  is the diameter of particles in the class  $i$ ;  $d_j$  is the diameter of particles in the class  $j$ .

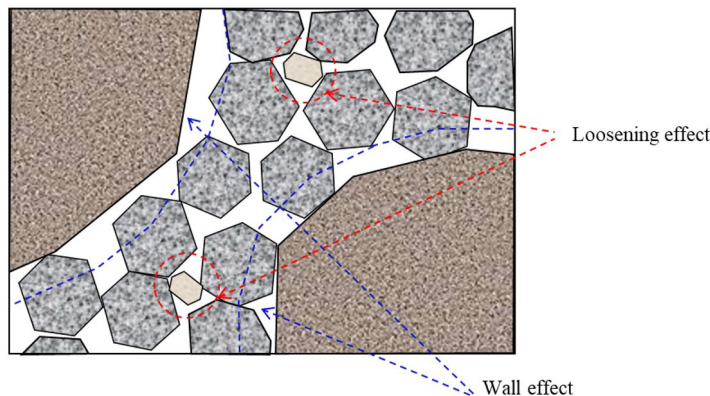


**Figure 1.** Loosening and wall effects between particles in a polydisperse mixture. Source: Adapted from Larrard [27].

Finally, the effect of the compaction energy on the packing density is considered in the modeling through the compaction index ( $K$ ), which expresses how much the real packing is close to the virtual packing and is calculated through the Equation 7. According to Larrard [30], as  $K$  tends to infinite number, the real packing density tends to virtual packing density. The author also recommends a  $K$  value of 14 for roller compacted concretes, 6.5 for self-compacting concretes and around 5 for normal vibrated concretes. Moreover, comparatively, it should be noted that in the case of dry concretes like RCC, compaction is a critical step for densification, whereas in the case of self-compacting concretes, which are flowable mixtures, the effect of interest is the shear deformation, as the mix gravity plays the main role in densification.

$$K = \sum_{i=1}^n \frac{\frac{\gamma_i}{\beta_i}}{\frac{1}{\Phi} - \frac{1}{\gamma_i}} \tag{7}$$

In the above equation  $K$  is the compaction index;  $y_i$  is the relative volume of material for each class;  $\beta_i$  is the packing density experimentally determined for each class;  $\gamma_i$  is the virtual packing density; and  $\Phi$  is the real packing density.

## 2 MATERIALS AND METHODS

The first step of the experimental study consisted of studying the particle size distributions regarding the theoretical models above described. Firstly, three particle size distributions from the bibliographic survey were picked up to analyze their modulus distribution (variable exponent in Equation 1). Afterward, it was determined three granulometric distributions falling into the limits for each grading curve to be analyzed regarding the models described by Equations 1 and 2, as well as the packing density in the CPM.

The particle size distributions were picked up thinking to meet the most used Brazilian, American and European specifications, which are: *Departamento de Estradas de Rodagem do Estado de São Paulo* (DER-SP) [17] CTCS specification, the European Standard EN 14227-1 [19] cement bound granular mixture 2 (maximum diameter of 20 mm) and the American Concrete Institute (ACI) [21] grading curve for RCC based on the United States Corps of Engineers (USACE) guide specification for RCC, and Pittman and Ragan’s [39] studies. These grading curves were also analyzed according to the empirical and analytical packing models and then three mixtures were produced to be analyzed through mechanical tests of compressive and indirect tensile strength. These steps are described in the flowchart depicted in Figure 2.

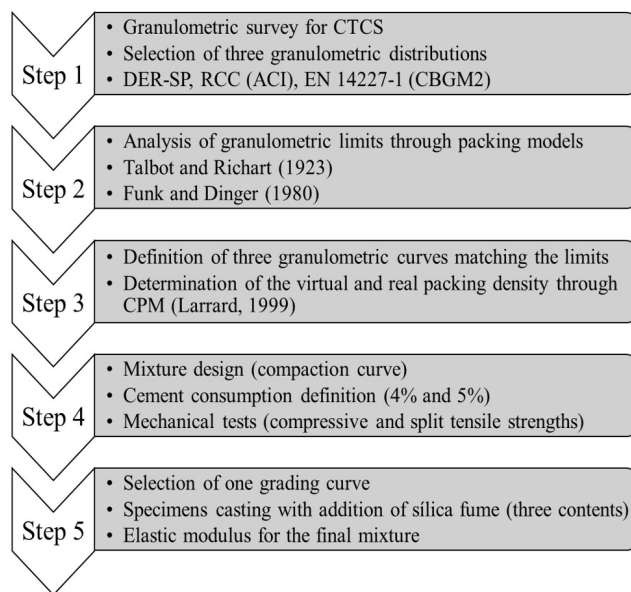


Figure 2. Flowchart of the experimental study

### 2.1 Analysis of the particle size distributions

The grading curves selected for analysis (DER-SP, ACI-RCC and EN-14227-1 CBGM2) are presented in Figure 3. Analysis on the particularities of each one and comparisons between them can be found in Cargnin et al. [15].

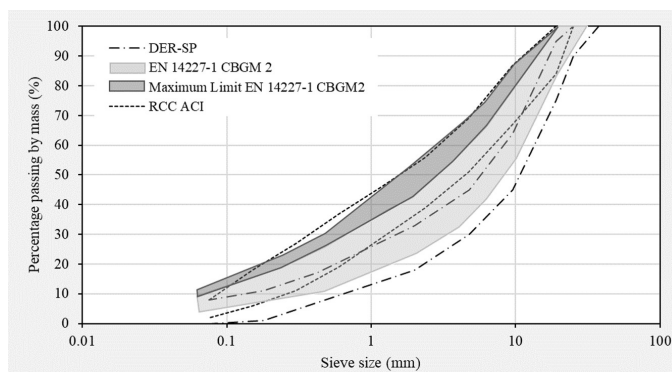


Figure 3. Particle size distributions considered

The remarkable differences among these curves depicted in Figure 3 are:

- ACI particle size distribution for RCC and DER-SP fulfill the EN 14227-1 (CBGM 2) excepting the DER-SP lower limit (coarse grading), which falls out of European standard limits. DER-SP fine grading is closer to the ACI-RCC coarse grading curve between sieves #9.5mm and #2.4mm highlighting the coarser grading permissiveness of CTCS.
- Whilst EN 14227-1 (CBGM 2) and ACI-RCC envelopes limit the maximum aggregate size in 20 mm and 19 mm, respectively, the DER-SP specification allows a maximum diameter of 25 mm.
- DER-SP specification limits the maximum percentage of fine aggregate in 45% (fraction passing through sieve #4.8mm), whereas the European standard allows a percentage around 80% of material passing through #4.8mm.
- Finally, while DER-SP tolerates 8% of filler (material passing through #0.075mm), EN 14227-1 (CBGM2) puts up with values around 18%; on the other hand, albeit ACI-RCC completely fits the EN 14227-1 limits, it is more restrictive regarding the filler fraction, limiting the percentage of material passing through #0.075mm in 12%, as the Pittman & Ragan RCC limits were developed seeking to minimize the material shrinkage.

Seeking to evaluate the packing density of these envelopes, their respective modulus of distribution was determined for the classical particle size distribution (Talbot & Richart) model and Funk & Dinger (Figures 4, 5 and 6).

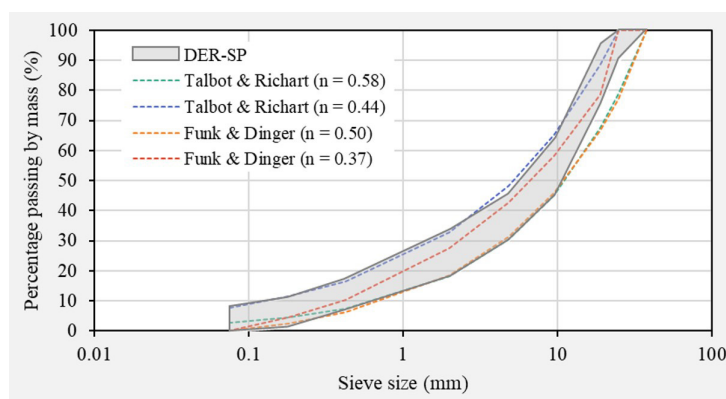


Figure 4. Distribution modulus calculated for DER-SP CTCS limits

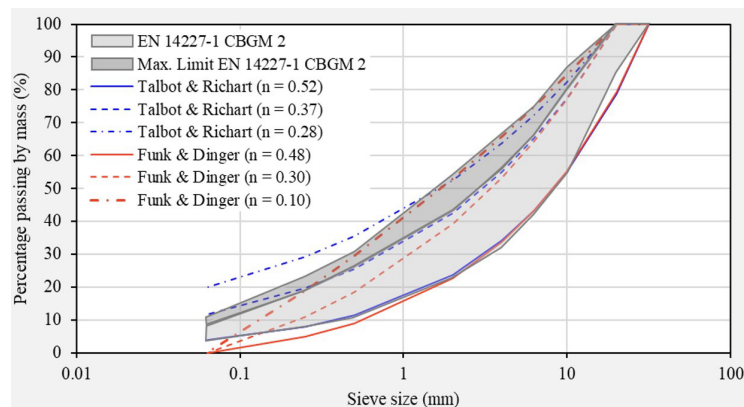
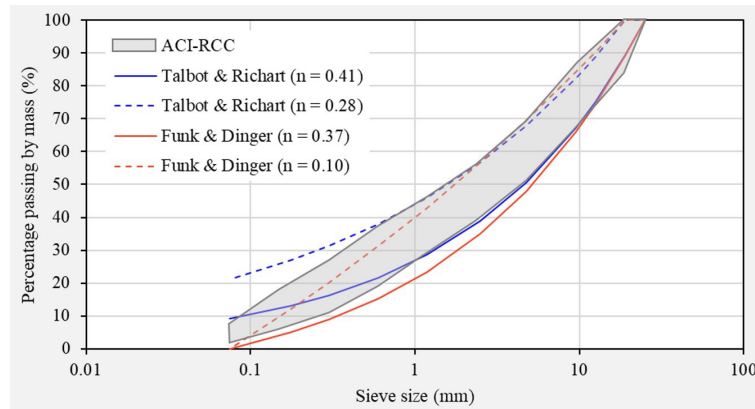


Figure 5. Distribution modulus calculated for EN 14227-1 CBGM2 limits



**Figure 6.** Distribution modulus calculated for ACI-RCC limits

From Figures 4, 5 and 6, the following comments can be inferred about the adjustment of the boundaries regarding the modulus of distribution ( $n$ ) of each curve for the Talbot & Richart and Funk and Dinger models:

- The modulus of distribution ( $n$ ) for Talbot & Richart model for DER-SP boundaries is 0.58 and 0.44 for the coarse and fine limits, respectively; for the coarse grading curve, however, the curve does not match between the fractions #25mm and #12.5mm, as well as below #0.42mm. Regarding the Funk & Dinger model, it is observed that  $n = 0.50$  almost matches the coarse curve except between fractions #25mm and #12.5mm, whilst the fine curve is far from the recommended  $n = 0.37$ . It is also observed that the curve tail is always zero since the model considers a minimum particle size.
- For EN 14227-1 (CBGM2) envelope, it is observed that  $n = 0.52$  almost matches the coarse limit, excepting fractions between #10mm and #20mm. For the fine limit,  $n = 0.37$  adjust the curve up to #0.5mm, then it is out and  $n = 0.28$  barely adjusts the curve for the maximum limit. The Funk & Dinger model adjusts well to the coarse curve only for  $n = 0.48$  exceeding the boundary below #2.0mm. The maximum limit, on the other hand, is well adjusted for  $n = 0.10$  up to #0.5mm, then the curve exceeds the boundary.
- The ACI-RCC coarse limit is well adjusted for  $n = 0.41$  (Talbot & Richart) until the fraction #1.18mm, then the ACI curve becomes more restrictive; the fine boundary is well adjusted for  $n = 0.28$  up to fraction #0.6mm. The Funk & Dinger model, conversely, does not adjust the boundaries for both boundaries.

From these analyses, three grading curves were picked up to develop three different mixtures analyzing their packing density by the CPM. The grading curves selected correspond to the DER-SP lower limit (fine gradation), CBGM 2 mean curve and ACI-RCC mean curve, as presented in the Figures 7, 8 and 9. In Figure 10, the three grading curves selected are plotted together in order to compare them.

These granulometric curves were picked up because of: (1) DER-SP fine limit is close to a mean curve for the CBGM 2 (EN 14227-1) and is one of the most used specifications for CTCS in Brazil; (2) CBGM 2 was the granulometric distribution selected among the several distributions from EN 14227-1 due to the requirement of a minimum compacity of 0.80 at the maximum modified Proctor dry density, expressed as the ratio between the absolute volume of solid and the apparent volume of the mixture; (3) the mean curve for RCC (ACI) is the target usually followed for RCC mixture design. It is observed in Figure 10 that the RCC mean curve is finer than the DER-SP lower limit and the CBGM 2 mean curve. Despite DER-SP and CBGM 2 curve are close, their granulometry slightly differ in the limit of fine aggregates (#4.8 mm), with the DER-SP presenting a slightly higher percentage of fine aggregates.

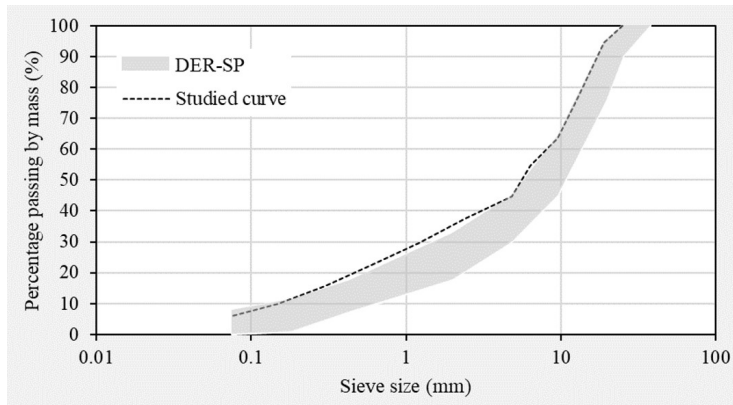


Figure 7. Studied grading curve matching DER-SP

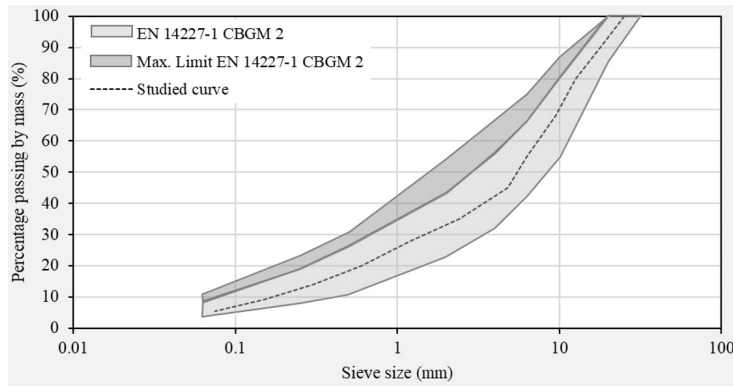


Figure 8. Studied grading curve matching CBGM 2 (EN 14227-1)

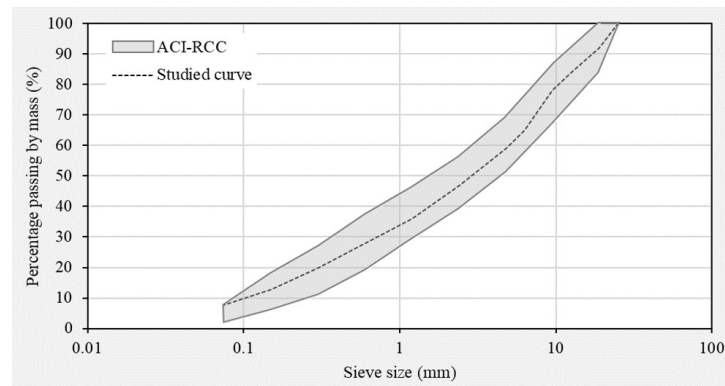


Figure 9. Studied grading curve matching ACI-RCC

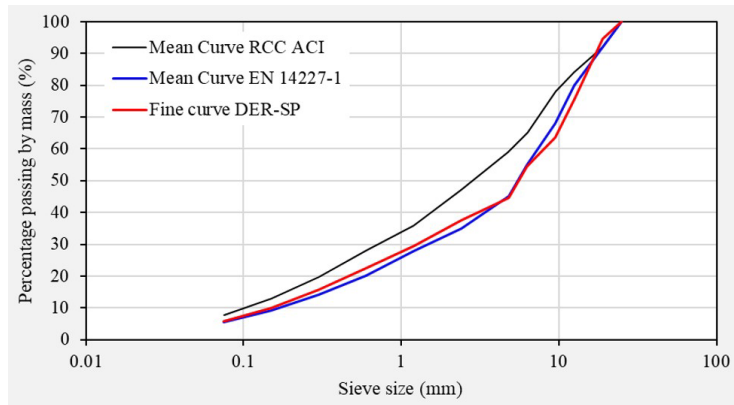


Figure 10. Studied grading curves together

### 2.1.1 Analysis of the packing density

To calculate the packing density according to the compressible packing model (CPM), the specific and unit mass for each fraction of aggregates separated through sieving process were determined; values are presented in Tables 2 and 3, respectively.

Table 2. Aggregates specific mass

Aggregate fraction	Specific mass (kg/m <sup>3</sup> )
Stone 1	2,670
Stone 0	2,790
Stone dust	2,640

Following the procedures in ABNT NBR 6458 [40] and DNER 195/97 [41]. Note: Stone 1 = maximum size of 19 mm; stone 0 = maximum size of 9.5 mm; stone dust = maximum size of 4.8 mm.

Table 3. Unit mass for each fraction of aggregates for determination of the real density packing through CPM

Aggregate diameter (mm)	Unit mass (kg/m <sup>3</sup> )	Packing density of the fraction
25.0	1,510	0.566
19.0	1,510	0.566
12.5	1,508	0.565
9.5	1,520	0.569
6.3	1,673	0.600
4.8	1,675	0.600
2.0	1,657	0.628
< 2.0	1,720	0.652

Following the procedures in ABNT NM 45 [42]

The virtual and real packing density were calculated by the Equations 4 and 7; the last one, as discussed, is influenced by the concrete densification process through the compaction index (K). The real packing density was then calculated assuming K = 14, as previously addressed, and it corresponds to the lowest value found as a solution for the equation, as presented in Figure 11.

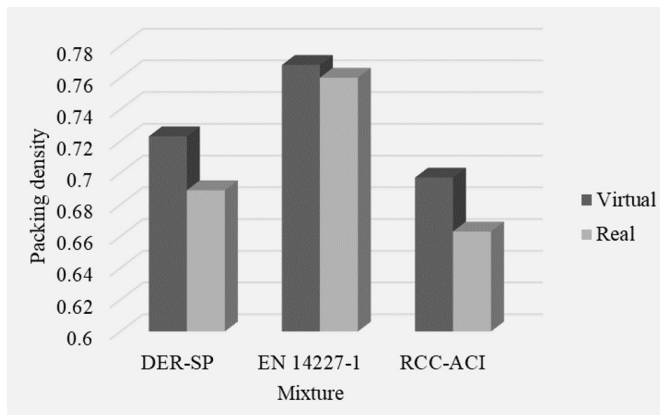


Figure 11. Virtual and real packing densities calculated for the selected mixtures

It is observed in Figure 11 that both the virtual and the real packing density for the EN 14227-1 mean grading curve are greater than those calculated for the DER-SP and RCC grading curves, suggesting the mix proportioning matching the European Standard specification could produce a mixture with a better packing and consequently improved strength. A previous study by Cargnin et al. [15] endorsed this assumption, showing that mixtures produced following EN 14227-1 mean grading curve presented compressive and indirect tensile strength 20% and 10%, respectively, greater than the DER-SP and ACI-RCC grading curves. Then, the EN 14227-1 CBGM 2 mean grading curve was selected as the more suitable granulometric distribution for the analysis of silica fume impact on the CTCS mechanical strength.

## 2.2 Mixture design

The mixture design was conducted seeking to determine the optimum moisture content and the maximum dry density, firstly for the mixtures without cement. Once the compaction curve was defined, the determination of the compaction moisture followed the recommendations issued by Balbo [7] to prepare the specimens with cement; they were compacted in the curve dry tail (moisture 1,5% below the optimum content) seeking to favor the crystals formation. The samples were compacted following the compaction test procedure recommended by the ABNT NBR 7182 [43]. They were prepared with two cement contents (4% and 5%) corresponding to cement consumptions nearby 95 and 120 kg/m<sup>3</sup>, respectively, and three different percentages of silica fume (5, 7, and 10%) added in relation of the cement mass.

The cement type used in this study corresponds to a CP III 40 sulfate resistant (SR), a blended or ternary cement produced with ground granulated blast furnace slag which content varies from 35% to 75%, limestone filler (up to 10%), beyond clinker and calcium sulfate, according to ABNT NBR 16697 [44]. The silica fume used is an aqueous solution where the silica is in suspension, favoring its handling and dispersion, especially in dry mixtures. The material particle size varies from 10 nm to 1 µm and its density is about 1.38. The cement characteristics and compaction curve are depicted in Table 4 and Figure 12, respectively.

Table 4. Cement characteristics and specifications

Characteristic	CP III SR 40
1-day compressive strength (MPa)	6.6
3-days compressive strength (MPa)	19.6
7-days compressive strength (MPa)	32.1
28-days compressive strength (MPa)	46.7
Initial setting time (min)	200
Blaine specific surface area (cm <sup>2</sup> )	4,812
Loss of ignition	1.16%
Calcium oxide (CaO)	52.53%
Silica (SiO <sub>2</sub> )	25.71%
Alumina (Al <sub>2</sub> O <sub>3</sub> )	8.32%
Iron oxide (Fe <sub>2</sub> O <sub>3</sub> )	1.91%
Magnesium oxide (MgO)	3.41%
Potassium oxide (K <sub>2</sub> O)	0.52%
Sulphate (SO <sub>3</sub> )	2.22%
Carbon dioxide (CO <sub>2</sub> )	3.18%
Insoluble residue	1.5%

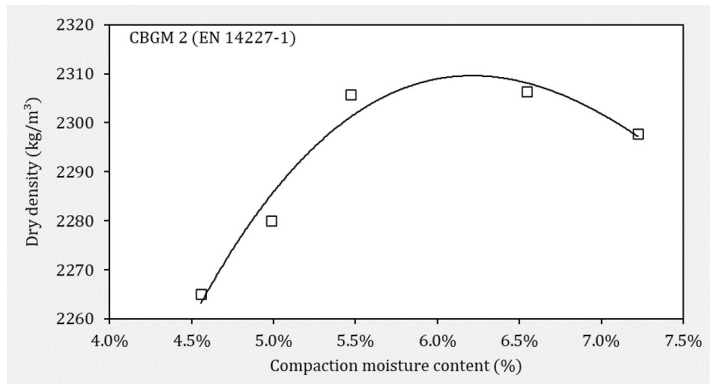


Figure 12. Compaction curves for CBGM2 (EN 14227-1) mean grading curve

### 2.3 CTCS Mechanical Parameters

Uniaxial compressive strength (NBR 5739 [45]) and indirect tensile strength (NBR 7222 [46]) of CTCS were assessed for 28 days of curing. The samples were kept in a closed box with temperature and moisture controlled, around 23°C and 80%, approximately, until end of curing time. Test was performed under a speed loading of 0.3 MPa/s for compressive strength whereas the indirect tensile strength used speed of 0.03 MPa/s, as recommended by standards. The modulus of elasticity was evaluated during indirect tensile tests measuring the specimen strain (at horizontal diameter) with a strain gauge as illustrated in Figure 13; the applied speed loading was 0.005 MPa/s to properly measure strains. The modulus of elasticity was also determined under compression following the recommendations of ABNT NBR 8522 and the ASTM C469 [47] to determine the Poisson’s ratio (Figure 13). The mixtures identification and the tests performed are described in Table 5; all tests were performed for a number of 6 specimens per mixture.

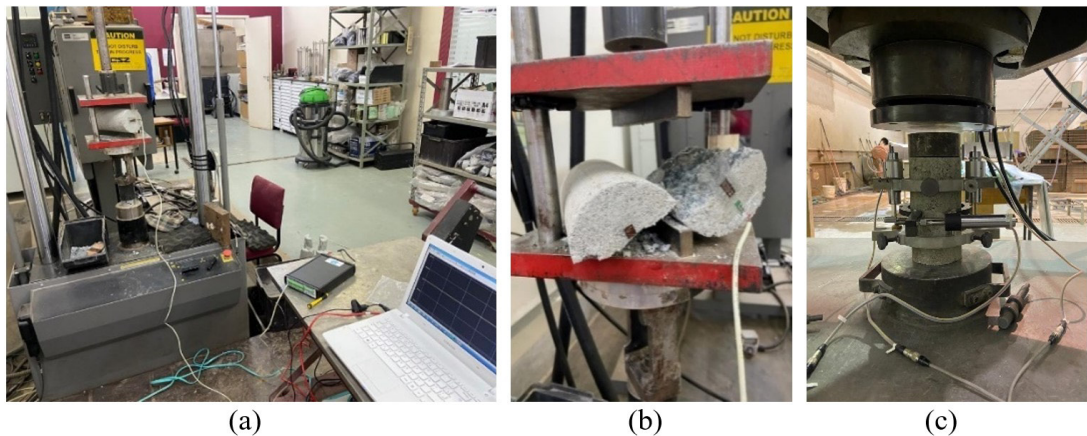


Figure 13. Data acquisition during the modulus of elasticity test: (a) specimen under splitting tensile; (b) specimen after rupture; (c) specimen under uniaxial compression

Table 5. Consumption of materials (kg/m³) for CTCS mix design projects

CTCS Mix	Cement	SF	Water	Sand	Gravel	Tests	No. of specimens
4% CPIII SR – C4	95	0	108.57	911.3	1,270.5	$f_{ct,sp}, f_c$	12
4% CP III SR + 5% silica fume – C4SF5	95	4.75	106.20	911.3	1,270.5	$f_{ct,sp}$	6
4% CP III SR + 7% silica fume – C4SF7	95	6.65	105.25	911.3	1,270.5	$f_{ct,sp}$	6
4% CP III SR + 10% silica fume – C4SF10	120	9.5	103.82	911.3	1,270.5	$f_{ct,sp}$	6
5% CPIII SR – C5	120	0	108.57	911.3	1,270.5	$f_{ct,sp}, f_c; E$ modulus	18
5% CP III SR + 5% silica fume – C5SF5	120	6.0	105.57	911.3	1,270.5	$f_{ct,sp}$	6
5% CP III SR + 7% silica fume – C5SF7	120	8.4	104.37	911.3	1,270.5	$f_{ct,sp}$	6
5% CP III SR + 10% silica fume – C5SF10	120	12.0	102.57	911.3	1,270.5	$f_{ct,sp}; E$ modulus	12

Note: CXSFY, where X is 4 or 5% (cement content) and Y is 5, 7, or 10% (silica fume content). The tests were performed considering 6 specimens per mixture per test.

### 3 RESULTS AND DISCUSSION

#### 3.1 Mechanical Strength

Figures 14 and 15 present the boxplot of data for compressive strengths of mixtures with 4% and 5% cement contents, as well as the indirect tensile strength for mixtures with different contents of silica fume.

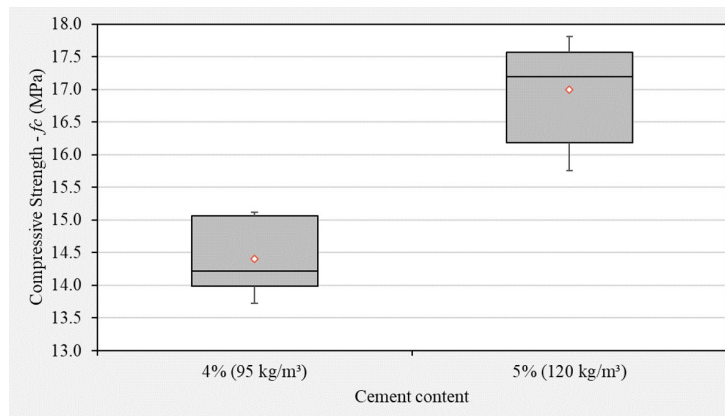


**Figure 14.** Boxplot of uniaxial compressive strength for mixtures with 4% and 5% cement

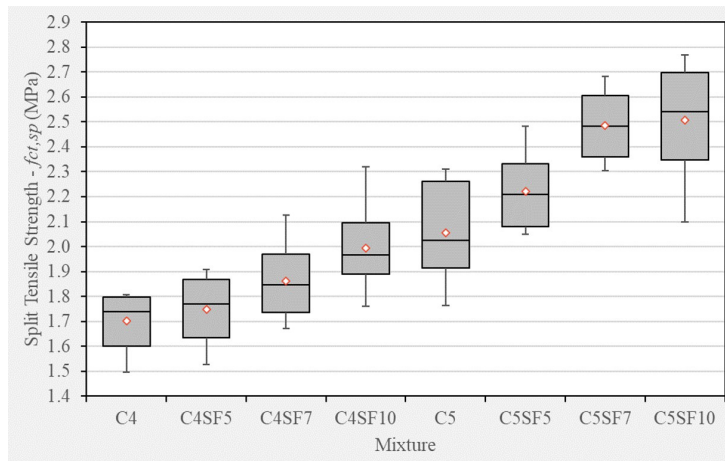


**Figure 15.** Boxplot of mixtures split tensile strength for mixtures with different contents of cement and silica fume. Note: CXSFY, where X is 4 or 5% (cement content) and Y is 5, 7, or 10% (silica fume content)

In Figure 14 a similar trend of dispersion of the results regarding the compressive strength is observed, with an asymmetry of the data. Regarding the split tensile strength (Figure 15), it can be noted that the dispersion of the results for both cement consumptions are similar. with a less variability for mixtures with 4% of cement. as depicted by the interquartile range. Additionally, there is a clear trend of symmetry in the split tensile results distribution, except for C5 mixture (shift in the middle of the box).

Seeking to evaluate the effectiveness of cement and silica fume content variation on the strength gain, hypothesis tests and analysis of variance (ANOVA) were performed. Firstly, a Test-F on the compressive and split tensile strengths for reference mixtures C4 and C5 was performed to confirm if the samples presented the same variance and then a T-student test was carried out to verify whether the average of the samples are indeed different. Both tests were conducted for a confidence level of 99% and the test results are summarized in Table 6.

**Table 6.** Hypothesis tests for mixtures with 4% and 5% of cement content

Parameter	Compressive strength ( $f_c$ )		Split tensile strength ( $f_{ct,sp}$ )	
	C4	C5	C4	C5
Mean (MPa)	14.41	17.00	1.70	2.06
Variance (MPa x MPa)	0.310	0.623	0.0146	0.0392
Standard Deviation (MPa)	0.556	0.789	0.121	0.198
Coefficient of variation	3.9%	4.6%	7.1%	9.6%
<i>Test-F</i>				
Observations	6		6	
Degree of freedom	5		5	
F-value	0.497		0.372	
p-value	0.230		0.151	
F <sub>critical</sub>	0.0911		0.0911	
Test Result	<i>Unequal variance</i>		<i>Unequal variance</i>	
<i>Test-t for mean difference of two samples with unequal variance</i>				
Mean difference hypothesis	0		0	
Degree of freedom	8		8	
Stat-t	-6.563		-3.724	
p-value (two tail test)	1.04E-04		5.83E-3	
t <sub>critical</sub> (two tail test)	3.250		3.355	

It is observed in Table 6 the average for both compressive and split tensile strengths are considered different for a significance level of 1%; when the cement consumption increases from 95 to 120 kg/m<sup>3</sup> the increment in the compressive and split tensile strength corresponds to 18% and 21%, respectively.

The effect of different silica fume content in tensile strength was analyzed; firstly, through a two-way ANOVA with replication for a confidence interval of 99% ( $\alpha = 0.01$ ). The null and alternative hypothesis assumed are described by Equation 8 as follows (results are presented in Table 7):

$$H_0 : \mu_1 = \mu_2 = \mu_3 \tag{8}$$

H<sub>a</sub>: at least one of the means is different

**Table 7.** ANOVA of the effect of cement and SF content on the indirect tensile strength

Source of variation	F-value	p-value	F <sub>critical</sub>
Cement content	100.84	1.71E-12	7.314
Silica content	12.22	8.13E-06	4.312
Interactions	1.31	0.283	4.312
$\alpha = 0.01$			

From Table 7 it can be inferred that the mean of the samples with different cement and silica fume contents differ by the F-value. However, when the interaction between the cement and silica fume content is analyzed, the ANOVA reveals the mean can be considered equal at least once. Then, t-Student hypothesis tests for a confidence level of 99% ( $\alpha = 0.01$ ) were performed to identify the ideal silica fume content which could promote a significant improvement in terms of strength (related to the reference mixtures C4 and C5), which results are presented in Table 8.

**Table 8.** t-Student hypothesis test for the difference of mean between samples

Parameter	C4	C4SF5	C4SF7	C4SF10
Mean	1.70	1.75	1.86	1.93
Variance	0.0146	0.0186	0.0240	0.00973
Standard deviation (MPa)	0.121	0.136	0.155	0.184
Coefficient of variation	7.1%	7.8%	8.3%	9.2%
No. specimens	6	6	6	5*
Mean difference hypothesis	-	0	0	0
Stat t	-	-0.634	-1.984	-3.417
p-value (two tail test)	-	0.540	0.078	0.00765
t <sub>critical</sub> (two tail test)	-	3.169	3.249	3.249

Parameter	C5	C5SF5	C5SF7	C5SF10
Mean	2.06	2.22	2.48	2.59
Variance	0.0392	0.0251	0.0184	0.0173
No. specimens	6	6	6	5*
Mean difference hypothesis	-	0	0	0
Stat t	-	-1.593	-4.381	-5.355
p-value (two tail test)	-	0.142	0.0017	4.59E-4
t <sub>critical</sub> (two tail test)	-	3.169	3.249	3.249

Parameter	C4SF7	C5	C5SF7	C5SF10
Mean	1.86	2.06	2.48	2.59
Variance	0.0204	0.0392	0.0184	0.0174
No. specimens	6	6	6	5
Mean difference hypothesis		0		0
Stat t		-1.885		-1.312
p-value (two tail test)		0.092		0.221
t <sub>critical</sub> (two tail test)		3.249		3.249

\*Outliers removed from boxplot analysis

Firstly, it is observed in Tables 6 and 8 the coefficient of variation is below 10% for all cases, endorsing the low dispersion of the results around the average and the data set homogeneity. Despite there is a trend of increasing the CTCS split tensile strength as the silica fume content increases (Figure 15), it should be noted in Table 8 that for cement content of 4% (95 kg/m<sup>3</sup>), the silica fume percentage that significantly impacts the mechanical strength compared to reference C4 is 10%; for mixtures C4SF5 and C4SF7, the hypothesis tests indicated the mean split tensile strength are considered equal. However, when the cement content increases to 5% (120 kg/m<sup>3</sup>), the content of silica that affects the tensile strength in a significant way is 7%, also compared to the reference mixture C5. In this case, the hypothesis test between the C5SF7 and C5SF10 mixtures reveals the means are considered equal.

Additionally, it is worth to highlight that in terms of mechanical strength, the increase of cement consumption from 4% to 5% could be compensated when 7% of silica fume is added to the mixture C4; the hypothesis test comparing the means of C4SF7 and C5 mixtures confirms they are equal for a confidence level of 99%.

The increment of mechanical strength of mixtures with silica addition is explained by the physical and chemical effect of the silica fume nanoparticles in the ITZ between the aggregate and the points where the cement paste promotes the bonding between the particles. The first one occurs due to the filler effect and paste densification, as silica fume particles act as nucleation points, contributing to formation of additional C-S-H. The chemical effect, on the other hand, is responsible for the C-S-H formation due to the reaction of silicon dioxide with the portlandite available in the porous solution from the silicate hydration.

### 3.2 Modulus of elasticity

Elasticity moduli were tested at 28 and 91 days for two mixtures (C5 and C5SF10); at 28 days the tests were conducted under unconfined compressive arrangement (also measuring the Poisson’s ratio) and diametral compression (C5 and C5SF10), whereas at 91 days the tests were performed just under diametral compression (C5SF10). Table 9 presents the results and in Figures 16 and 17 are presented, the test results boxplot and the stress *versus* strain curves under diametral compression, respectively.

**Table 9.** Modulus of elasticity and Poisson’s ratio results

Compressive test									
Mixture	Age (days)	# specimens	$E$ (MPa)	sd (MPa)	cv	$\nu$	sd	cv	
C5SF10	28	6	19,285	966	5%	0.203	0.034	17%	
Split Test									
Mixture	Age (days)	# specimens	$E_{cs}^*$ (MPa)	sd (MPa)	cv	$E^{**}$ (MPa)	sd (MPa)	cv	
C5SF10	28	3	23,092	1,610	7%	18,508	1,720	9.3%	
C5SF10	91	6	24,677	2,715	11%	17,276	1,862	11%	
C5	28	6	24,715	3,002	12.1%	17,617	1,189	7%	

\*Secant elastic modulus at 0%-30% of  $f_{ct,sp}$ ; \*\*Secant elastic modulus at 30%-100% of  $f_{ct,sp}$ .

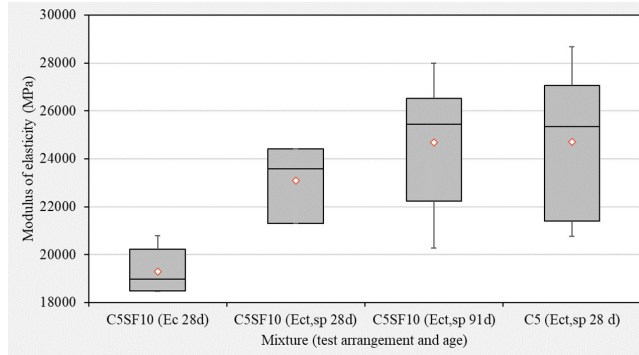
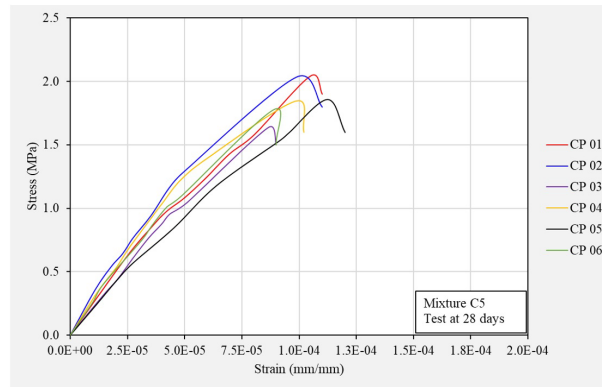
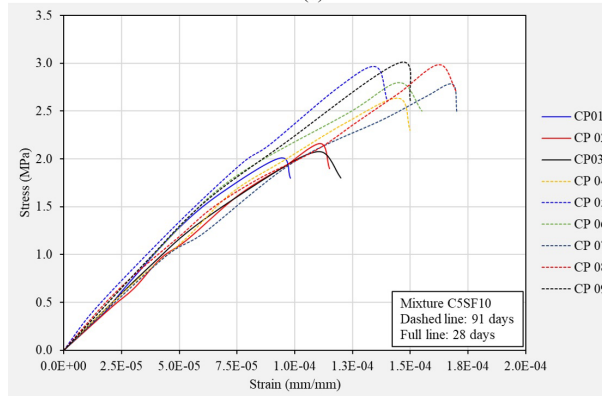


**Figure 16.** Modulus of elasticity boxplot



(a)



(b)

**Figure 17.** Stress versus strain curves: (a) C5 (5% of cement without silica fume) at 28 days; (b) C5SF10 (5% of cement and 10% of silica fume) at 28 and 91 days.

It is observed from Figure 16 that although there is some asymmetry in the boxes, the mean values are close to the median; t-Student hypothesis tests for mean difference at a confidence level of 99% confirmed equality of modulus of elasticity for both mixtures as depicted in Table 10. In Figure 17, it is verified that the shape of the stress-strain ( $\sigma$ - $\epsilon$ ) curve under diametral compression has a linear trend pointing to the elastic-linear behavior of the material in tensile as stated by Balbo and Badawy [48]. However, when the stress level is close to the ultimate stress, the rupture is abrupt, revealing the extremely brittle nature of CTCS. Nevertheless, the ultimate stress and strain for mixtures with 10% of silica fume at 91 days are greater than those values obtained for the reference mixture (C5).

**Table 10.** t-Student hypothesis test for modulus of elasticity of CTCS

Parameter	C5	C5SF10 28d*	C5SF10 91d*	C5SF10 91d**
Mean	24.715	23.091	24.677	24.677
Variance	9,009,856	2,592,129	7,372,810	7,372,810
# specimens	6	3	6	6
Mean difference hypothesis	-	0	0	0
Stat t	-	-1.056	-0.023	-1.096
p-value (two tail test)	-	0.326	0.982	0.315
t <sub>critical</sub> (two tail test)	-	3.499	3.169	3.707

\*Comparison with the reference C5; \*\*Comparison with C5SF10 at 28 days.

Balbo [7] addressed that, under uniaxial compression, the CTCS is strongly dependent on the aggregate distribution in the mixture. To understand this statement, it should be noted that cementitious materials are a composite which mechanical response, especially the modulus of elasticity, is in the halfway between the aggregate (about 60 GPa) and the cement paste (around 15 to 20 GPa, depending on the water-cement ratio, hydration degree, air content, etc.). Under compression, the stress-strain curve is characterized by an elastic-linear trend up to 30% of the load breaking; between 30% and 50%, the internal microcracks in the ITZ, which are still stable, grow up causing a deviation in the  $\sigma$ - $\epsilon$  diagram. Above this level, the internal cracks raise until they become unstable and then the rupture occurs quickly.

Under tensile, on the other hand, although the grains distribution is relevant to the mixture split tensile strength ( $f_{ct,sp}$  is greater for mixtures with greater aggregate packing as demonstrated by Carginin et al. [15]), the modulus of elasticity does not seem to be significantly influenced by the granulometric distribution, since under this arrangement the cement paste, responsible for the aggregate punctual bonding, is the main portion that rules the modulus of elasticity, as depicted in Figure 18.

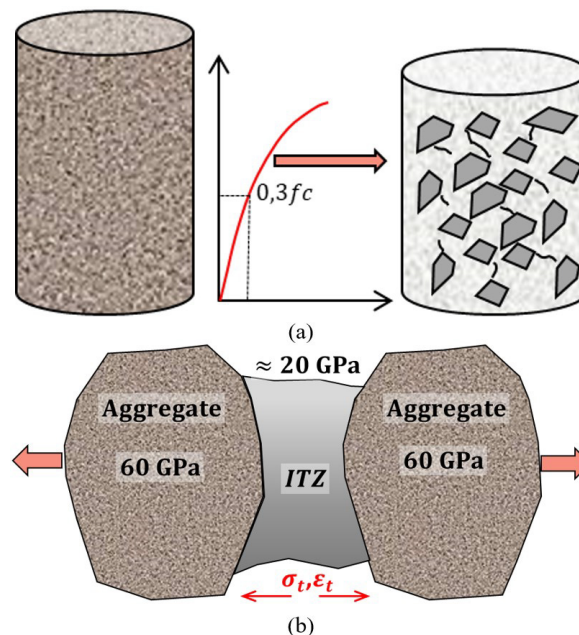


**Figure 18.** Illustration of modulus of elasticity measurement: (a) in compression; (b) in indirect tensile.

Additionally, Balbo (1993) obtained modulus of elasticity values under split tensile around 22,007 MPa (CV = 6.3%) and  $f_{ct,sp}$  of 2.33 MPa (CV = 15%) for conventional standard CTCS with 4% of CP II-E 32 at 56 days and particle size distributions falling in the boundaries specified in the ABNT NBR 11803 range B, resulting in a  $E_{t,sp}/f_{ct,sp}$  relationship around 9,445. It is worth to comment that CP II-E is a cement with ground-granulated blast furnace slag as supplementary cementitious material replacing the clinker, like CP III, but the percentage of slag in the first is lower than the last. While CP II-E may contain a slag percentage between 6 and 34%, CP III may contain from 35% up to 75% of slag. It reflects some difference of strength in the first days of cure. However, after 28 days, the strengths are similar.

In this study, conversely, the CTCS using the CBGM2 EN 14227-1 limits (which leads to a better aggregate packing) with cement content of 5% (CP III SR 40) and addition of 10% of silica fume, lead to  $E_{t,sp}$  and  $f_{ct,sp}$  values, at 91 days, of 24,677 (CV = 11%) and 3.0 MPa (CV = 8%), respectively, reaching modular relationship of 8,200, approximately. Comparing current results,  $E_{t,sp}/f_{ct,sp}$  obtained for the reference mixture (C5) was about 12,000. From the point of view of structural response, a reduced modular relationship is a huge positive outcome, as it can improve the fatigue behavior of the material which is ruled by the stress-strength ratio ( $SSR = \sigma_t/f_{ct,sp}$ ).

Average compressive modulus of elasticity was similar to values suggested by Balbo (1993) for CTCS with 4% of cement content – 20,134 MPa with  $cv = 12.6\%$ . Comparing the values obtained in compression and indirect tensile, hypothesis test for mean difference for a confidence level of 99% confirmed the average are considered equal at 28 days, with  $Stat\ t = 3.690$  and  $t_{critical} = 5.841$  ( $p\text{-value} = 0.032$ ).

Regarding the Poisson's ratio, the values obtained were closest to the values typically obtained for conventional dry concretes (close to 0.20). However, it was observed an important variability of the results (CV = 17%), despite the low variability obtained in the modulus tests, as both parameters are measured simultaneously.

#### 4 CONCLUSIONS

This study sought to contribute to the formulation of an innovative high-performance cement-treated crushed stone (HP-CTCS) based on improvements of the particle size distribution and addition of a supplementary cementitious material capable of modifying the interfacial transition zone (ITZ) in the cement paste punctual bonding. Then, an extensive experimental schedule was settled embracing the analysis and selection of a suitable grading curve, as well as the preparation of samples with two cement contents (4% and 5%) and different percentages of silica fume (5, 7 and 10% of the cement mass) to investigate their mechanical properties. The analysis of test results allows to summarize the main findings as follows:

- The analysis of the selected grading curves according to the Talbot & Richart classical particle size distribution, as well as the compressible packing model indicated the mean grading curve for the EN 14227-1 (CBGM 2) is better packed than the DER-SP fine gradation and the mean curve for ACI-RCC, resulting in a mixture with compressive and split tensile strengths higher (20% and 10% respectively) than the other two curves.
- The optimum content of emulsified silica fume for mixtures with 4% and 5% cement content is 10% (by cement mass). Moreover, the increase in the split tensile strength obtained by increasing the cement content from 4% to 5% (mixtures without SF) can be compensated in mixture C4 by adding 7% of silica fume (by cement mass).
- The impact of producing HP-CTCS with 5% cement content and 10% silica fume increased the split tensile strength in approximately 30%, compared to conventional CTCS, whilst the impact on the elastic modulus was only 12%, leading to a reduction of 35% in the modular relationship. This is a positive outcome regarding the material fatigue performance, since fatigue life is ruled by the stress-strength relationship ( $SSR = \sigma_t/f_{ct,sp}$ ), making the HP-CTCS a material potentially more durable than the conventional CTCS. The Poisson's ratio for CTCS was similar to the values obtained for dry and plastic concretes (0.20). However, the high variability (17%) of tests reveals the complexity of repeatability of the test.

Future analyzes (currently in course) on the fatigue and fracture behavior of HP-CTCS studied may allow advancing even more on the microstructural behavior of these materials, as well as setting fatigue models for them. The results obtained with minimum costs impacts for actual construction sites disclosed the perspectives on the use of high-performance CTCS, comparable to RCC, in order to improve field durability for road and airport semi-rigid pavements.

#### ACKNOWLEDGEMENTS

The authors thank to CAPES (Coordination for the Improvement of Higher Education Personnel) for the scholarship provided for the first author and the following partners: Lafarge-Holcim Brazil (CSN) for supplying aggregates and cement. and Tecnosil for supplying the silica fume in suspension.

## REFERENCES

- [1] E. J. Yoder and M. W. Witzczak, *Principles of Pavement Design*, 2nd ed. New York, NY, USA: Wiley, 1975.
- [2] S. Lim and D. G. Zollinger, "Estimation of the compressive strength and modulus of elasticity of cement-treated aggregate base materials," *Transp. Res. Rec.*, vol. 1837, no. 1, pp. 30–38, Jan. 2003, <http://dx.doi.org/10.3141/1837-04>.
- [3] P. Saxena, D. Tompkins, L. Khazanovich, and J. T. Balbo, "Evaluation of characterization and performance modeling of cementitiously stabilized layers in the Mechanistic-Empirical pavement design guide," *Transp. Res. Rec.*, vol. 2186, no. 1, pp. 111–119, Jan. 2010, <http://dx.doi.org/10.3141/2186-12>.
- [4] D. X. Xuan, L. J. M. Houben, A. A. A. Molenaar, and Z. H. Shui, "Mechanical properties of cement-treated aggregate material - a review," *Mater. Des.*, vol. 33, pp. 496–502, Jan. 2012, <http://dx.doi.org/10.1016/j.matdes.2011.04.055>.
- [5] P. Wu, *Cement-Bound Road Base Materials, Report 7-11-218-1*. Delft, The Netherlands: Delft Univ./PowerCem Technol., 2011.
- [6] D. York, "Cement-bound materials (CBM)," in *Advanced Concrete Technology*, vol. 4, J. Newman and B. S. Choo, Eds., Oxford, UK: Elsevier, 2003, pp. 1–12. <http://dx.doi.org/10.1016/B978-075065686-3/50309-8>.
- [7] J. T. Balbo, "Estudo das propriedades mecânicas das misturas de brita e cimento e sua aplicação aos pavimentos semi-rígidos," Doctor of Science dissertation, Esc. Polít., Univ. São Paulo, São Paulo, 1993.
- [8] F. S. Albuquerque and A. T. Mendonça, "Análise crítica e ajuste de modelos de previsão de fadiga com análise incremental de danos para BGTC executada em pavimento asfáltico semirrígido," *Transportes*, vol. 25, no. 2, pp. 107–123, Aug. 2017, <http://dx.doi.org/10.14295/transportes.v25i2.1046>.
- [9] R. S. Nascimento and F. S. Albuquerque, "Estudo de desempenho à fadiga de base cimentada tipo BGTC na BR-101/SE," *Transportes*, vol. 26, no. 1, pp. 21–36, Apr. 2018, <http://dx.doi.org/10.14295/transportes.v26i1.1358>.
- [10] J. T. Balbo, "Britas graduadas tratadas com cimento: uma avaliação de sua durabilidade sob o enfoque de porosidade, tenacidade e fratura," *Transportes*, vol. 14, no. 1, pp. 45–53, Jul. 2006, <http://dx.doi.org/10.14295/transportes.v14i1.59>.
- [11] P. Sherwood, *Soil Stabilization with Cement and Lime: State of the Art Review*. London, UK: TRL, 1993.
- [12] S. Chakrabarti and J. Kodikara, "Basaltic crushed rock stabilized with cementitious additives: compressive strength and stiffness, drying shrinkage, and capillary flow characteristics," *Transp. Res. Rec.*, vol. 1819, no. 1, pp. 18–26, Jan. 2003, <http://dx.doi.org/10.3141/1819b-03>.
- [13] J. Piratheepan, C. T. Gnanendran, and S.-C. R. Lo, "Characterization of cementitiously stabilized granular materials for pavement design using unconfined compression and IDT testings with internal displacement measurements," *J. Mater. Civ. Eng.*, vol. 22, no. 5, pp. 495–505, Oct. 2009, [https://doi.org/10.1061/\(ASCE\)MT.1943-5533.000005](https://doi.org/10.1061/(ASCE)MT.1943-5533.000005).
- [14] J. LaHucik and J. Roesler, "Field and laboratory properties of roller-compacted concrete pavements," *Transp. Res. Rec.*, vol. 2630, no. 1, pp. 33–40, Jan. 2017, <http://dx.doi.org/10.3141/2630-05>.
- [15] A. P. Carginin, J. T. Balbo, and L. L. B. Bernucci, "Efeito de diferentes granulometrias normativas na resistência mecânica de concretos compactados com rolo para pavimentação," *Concr. Constr.*, vol. 108, no. 4, pp. 28–36, Dec. 2022.
- [16] Associação Brasileira de Normas Técnicas, *Materiais para Base ou Sub-Base de Brita Graduada Tratada com Cimento – Requisitos*, NBR 11803, 2013.
- [17] Departamento de Estradas de Rodagem do Estado de São Paulo, *Sub-Base ou Base de Brita Graduada Tratada com Cimento – BGTC*, ET-DE-P00/009, 2005.
- [18] Departamento de Estradas de Rodagem do Estado do Paraná, *Pavimentação: Brita Graduada Tratada com Cimento*, ES-P 16/05, 2005.
- [19] Comité Européen de Normalisation, *Hydraulically Bound Mixtures - Specifications - Part 1: Cement Boud Granular Mixtures*, EN 14227-1, 2013.
- [20] Portland Cement Association, *Guide to Cement-Treated Base (CTB)*. Washington, DC, USA: Portland Cement Assoc., 2006.
- [21] American Concrete Institute, *Report on Roller-Compacted Concrete Pavements*, ACI 325.10R-95, 2001.
- [22] P. K. Mehta and P. J. M. Monteiro, *Concreto: Microestruturas e Materiais*. São Paulo: IBRACON, 2008.
- [23] A. M. Neville and J. J. Brooks, *Tecnologia do Concreto*, 2nd ed. Porto Alegre: Bookman, 2010.
- [24] K. L. Scrivener, A. K. Crumbie, and P. Laugesen, "The interfacial transition zone (ITZ) between cement paste and aggregate in concrete," *Interface Sci.*, vol. 12, no. 4, pp. 411–421, Oct. 2004, <http://dx.doi.org/10.1023/B:INTS.0000042339.92990.4c>.
- [25] J. Marchand, H. Hornain, S. Diamond, M. Pigeon, and H. Guiraud, "The microstructure of dry concrete products," *Cement Concr. Res.*, vol. 26, no. 3, pp. 427–438, Mar. 1996, [http://dx.doi.org/10.1016/S0008-8846\(96\)85030-7](http://dx.doi.org/10.1016/S0008-8846(96)85030-7).
- [26] F. Vahedifard, M. Nili, and C. L. Meehan, "Assessing the effects of supplementary cementitious materials on the performance of low-cement roller compacted concrete pavement," *Constr. Build. Mater.*, vol. 24, no. 12, pp. 2528–2535, Dec. 2014, <http://dx.doi.org/10.1016/j.conbuildmat.2010.06.003>.
- [27] F. Larrard, "Concrete mixture proportioning: a scientific approach," in *Modern Concrete Technology Series*, A. Bentur and S. Mindess, Eds., London, UK: E. & F.N. Spon, 1999, pp. 1–403.

- [28] H. F. Campos, "Dosagem de concreto sustentável de alta resistência, otimizada por modelos de empacotamento de partículas, com substituição parcial do cimento Portland por pó de pedra e sílica ativa," Doctoral dissertation, Univ. Fed. Paraná, Curitiba, 2019.
- [29] S. A. A. M. Fennis, "Design of ecological concrete by particle packing optimization," Doctoral dissertation, Fac. Civil Eng. Geosci., Delft Univ. Technol., Delft, The Netherlands, 2011.
- [30] F. Larrard, "Concrete optimisation with regard to packing density and rheology," in *3rd RILEM Int. Symp. Rheol. Cement Suspens. Fresh Concr.*, 2009, pp. 1–8.
- [31] C. Londero, "Dosagem de concreto ecológico com base em estudo de empacotamento de partículas," Master thesis, Univ. Fed. Paraná, Curitiba, 2016.
- [32] S. V. Kumar and M. Santhanam, "Particle packing theories and their application in concrete mixture proportioning: a review," *Indian Concr. J.*, vol. 77, no. 9, pp. 1324–1331, 2003.
- [33] M. Glavind and C. Much-Petersen, "Green concrete - a life cycle approach," in *Proc. Challen. Concr. Constr.*, 2002, pp. 01–16.
- [34] W. B. Fuller and S. E. Thompson, "The laws of proportioning concrete," *Trans. Am. Soc. Civ. Eng.*, vol. 59, no. 2, pp. 67–143, Dec. 1907.
- [35] A. N. Talbot and F. E. Richart, *The Strength of Concrete - Its Relation to the Cement Aggregates and Water*. Urbana-Champaign, IL, USA: Univ. Illinois, 1923.
- [36] A. H. M. Andreasen and J. Andersen, "Ueber die beziehung zwischen kornstufung und Zwischenraum in produkten aus losen Körnern (mit einigen experimenten)," *Colloid Polym. Sci.*, vol. 50, no. 3, pp. 217–228, 1930.
- [37] R. D. Vanderlei, "Análise experimental do concreto de pós reativos: dosagem e propriedades mecânicas," Doctoral dissertation, Esc. Eng. São Carlos, Univ. São Paulo, São Carlos, 2004.
- [38] J. E. Funk and D. R. Dinger, *Grinding and Particle Size Distribution Studies for Coal-Water Slurries at High Solids Content. Final Report*. ESEERCO, 1980.
- [39] D. W. Pittman and S. A. Ragan, "Drying shrinkage of roller-compacted concrete for pavement applications," *ACI Mater. J.*, vol. 95, no. 1, pp. 19–26, Jan./Feb. 1998.
- [40] Associação Brasileira de Normas Técnicas, *Grãos de Pedregulho Retidos na Peneira de Abertura 4,8 Mm - Determinação da Massa Específica Aparente e da Absorção de Água*, NBR 6458, 2016.
- [41] Departamento Nacional de Estradas de Rodagem, *Agregados - Determinação da Absorção e da Massa Específica de Agregado Graúdo*, DNER-ME 195/97, 1997.
- [42] Associação Brasileira de Normas Técnicas, *Agregados - Determinação da Massa Unitária e do Volume de Vazios*, NBR NM 45, 2009.
- [43] Associação Brasileira de Normas Técnicas, *Solo - Ensaio de Compactação*, NBR 7182, 2016.
- [44] Associação Brasileira de Normas Técnicas, *Cimento Portland - Requisitos*, NBR 16697, 2018.
- [45] Associação Brasileira de Normas Técnicas, *Concreto - Ensaio de Compressão de Corpos-de-Prova Cilíndricos*, NBR 5739:2007, 2018.
- [46] Associação Brasileira de Normas Técnicas, *Compressão Diametral*, NBR 7222, 2011.
- [47] American Society for Testing Materials, *Standard Test Method for Static Modulus of Elasticity and Poisson's Ratio of Concrete in Compression*, ASTM C469/C469M-10, 2010. [http://dx.doi.org/10.1520/C0469\\_C0469M-10](http://dx.doi.org/10.1520/C0469_C0469M-10).
- [48] J. T. Balbo and M. Badawy, "Britas tratadas com cimento: elasticidade linear ou não linear?" in *An. 7th Enc. Assoc. Nac. Ens. Pesq. Transp.*, 1993, pp. 915–922.

---

**Author contributions:** APC: laboratory work, samples preparation, testing, analysis, and writing; JTB: advising, supervision, analysis, review; LLBB: co-advising, supervision, analysis, review.

**Editors:** Diogo Ribeiro, Guilherme Aris Parsekian.